Temporal Decoding by Phase-Locked Loops: Unique Features of Circuit-Level Implementations and Their Significance for Vibrissal Information Processing

Miriam Zacksenhouse
memz@tx.technion.ac.il
Sensory-Motor Integration Laboratory, Technion Institute of Technology, Haifa, Israel

Ehud Ahissar
ehud.ahissar@weizmann.ac.il
Department of Neurobiology, Weizmann Institute, Rehovot, Israel

Rhythmic active touch, such as whisking, evokes a periodic reference spike train along which the timing of a novel stimulus, induced, for example, when the whiskers hit an external object, can be interpreted. Previous work supports the hypothesis that the whisking-induced spike train entrains a neural implementation of a phase-locked loop (NPLL) in the vibrissal system. Here we extend this work and explore how the entrained NPLL decodes the delay of the novel, contact-induced stimulus and facilitates object localization. We consider two implementations of NPLLs, which are based on a single neuron or a neural circuit, respectively, and evaluate the resulting temporal decoding capabilities. Depending on the structure of the NPLL, it can lock in either a phase- or co-phase-sensitive mode, which is sensitive to the timing of the input with respect to the beginning of either the current or the next cycle, respectively. The co-phase-sensitive mode is shown to be unique to circuit-based NPLLs. Concentrating on temporal decoding in the vibrissal system of rats, we conclude that both the nature of the information processing task and the response characteristics suggest that the computation is sensitive to the co-phase. Consequently, we suggest that the underlying thalamocortical loop should implement a circuit-based NPLL.

1 Introduction

One of the major computational tasks facing the vibrissal somatosensory system is to determine the angle of the vibrissa on contact with an external obstacle. The vibrissal system receives external sensory input from the trigeminal neurons whose response patterns include both whisking locked spikes and contact-induced spikes (Szwed, Bagdasarian, & Ahissar, 2003). The whisking locked spike train provides a periodic reference input at the whisking frequency. The contact-induced activity represents the

timing of the novel event of interest. When whisking frequency is consistent across cycles, the resulting computational task is equivalent to decoding the temporal delay or phase shift of a novel input with respect to a reference periodic input (Ahissar & Zacksenhouse, 2001), a basic computational task shared by other active sensory tasks, including vision (Ahissar & Arieli, 2001).

At the algorithmic level (Marr, 1982), it was suggested that this computation can be performed by phase-locked loops (PLL) (Ahissar & Vaadia 1990; Ahissar, Haidarliu, & Zacksenhouse, 1997; Ahissar & Zacksenhouse, 2001). PLLs are (electronic) circuits that can lock to the frequency of their external input and perform important processing tasks, including frequency tracking and demodulation (Gardner, 1979). One of the major motivations for this hypothesis is based on the implementation level. Specifically, neuronal implementations of circuit-based PLLs (NPLLs), like the one shown in Figure 1 and detailed in section 2, require neuronal oscillators whose frequencies can be controlled by the input rate (rate-controlled oscillator, RCO) (Ahissar et al., 1997; Ahissar, 1998). Thus, the evidence that over 10% of the individual neurons in the somatosensory cortex can operate as controllable neural oscillators (Ahissar et al., 1997; Ahissar & Vaadia, 1990; Amitai, 1994; Flint, Maisch, & Kriegstein, 1997; Lebedev & Nelson, 1995; Nicolelis, Baccala, Lin, & Chapin, 1995; Silva, Amitai, & Connors, 1991) provided the initial motivation and further support for the hypothesis that these neurons function as RCOs in circuit-based NPLLs.

Other requirements for implementing PLLs in the vibrissal system and agreement with the model predictions have also been demonstrated:

- The frequencies of the local cortical oscillators can be increased by local glutamatergic excitation (Ahissar et al., 1997).

- These oscillators can track the whisker frequency (Ahissar et al., 1997).

- The whisker frequency is encoded in the latency of the response of thalamic neurons (Ahissar, Sosnik, & Haidarliu, 2000; Sosnik, Haidarliu, & Ahissar, 2001).

- Thalamic neurons respond after (and not before, as would be expected from relay neurons) cortical neurons (Nicolelis et. al, 1995) as predicted by a thalamocortical PLL (Ahissar et al., 1997).

While these investigations focused on the response of the vibrissal system to the reference, whisking-induced input, the response to the novel contact-induced input was not investigated in detail. The purpose of this article is to investigate and demonstrate how NPLLs respond to the novel contact-induced input and assess the resulting temporal decoding capabilities. Furthermore, we address the issue of whether circuit-based NPLLs provide any computational advantages over single-neuron implementations (Hoppensteadt, 1986). Specifically, we distinguish between two

locking modes, which are sensitive to either the phase or co-phase of the input (the normalized delay of the input with respect to the preceding or succeeding oscillatory event, respectively). It is shown that single neurons can implement only phase-sensitive NPLLs, while circuit-based NPLLs can implement both. In the context of the vibrissal thalamocortical system, both the response characteristics and the nature of the information processing task suggest that the computation should be sensitive to the co-phase and thus should be implemented by circuit-based NPLLs.

Section 2 develops a mathematical model of NPLLs and describes four possible variants and their respective characteristics. Section 3 investigates the temporal decoding capabilities provided by the different NPLLs and evaluates them with respect to the temporal decoding task performed by the vibrissal system. Section 4 investigates the response characteristics of cortical oscillators and determines which of the four NPLL variants they implement. The information processing capabilities of NPLLs implemented by single neural oscillators and by neural circuits are discussed in section 5, considering both temporal decoding and temporal pattern generation.

2 Mathematical Modeling of PLLs

Different neuronal implementations of the well-known electronic PLLs (Gardner, 1979) are possible (Ahissar, 1998), including for example, the neuronal circuit of Figure 1. The instantaneous frequency of the neural oscillator depends on its intrinsic frequency and the rate of its input (rate-controlled oscillator, RCO). The input to the RCO is generated by an ensemble of phase-detecting neurons, grouped together as a PD, whose ensemble output rate depends on the delay between the external spike and the RCO-evoked spike. When the NPLL locks to the external input, the instantaneous frequency of the internal RCO tracks the instantaneous frequency of the external input, and the deviation from the intrinsic frequency is encoded in the output rate of the PD (Ahissar et al., 1997; Ahissar, 1998).

2.1 Phase Models. The activity of a neural oscillator may involve a single spike or a burst of spikes, which repeat periodically. It is natural to describe the periodic activity as a function of a phase variable (Rand, Cohen, & Holmes, 1986). By normalizing the phase of the oscillator $\theta_{osc}(t)$ to a unit interval, that is, $\theta_{osc} \in [0, 1]$, it describes the fraction of the elapsed cycle. When the phase reaches the unit level, it resets to zero, and the oscillator generates a single spike or a burst of spikes. The phase of a free oscillator varies at a constant rate, whose inverse determines its intrinsic period τ_{osc}. So: $\dot{\theta}_{osc} = \tau_{osc}^{-1}$ (Zacksenhouse, 2001).

The input to the oscillator affects the rate at which the phase changes and thus the period of the oscillator. In general, the effect may depend on the complete history of the input. However, here we assume that upon completing an oscillatory cycle and generating a spike in the case of a neural
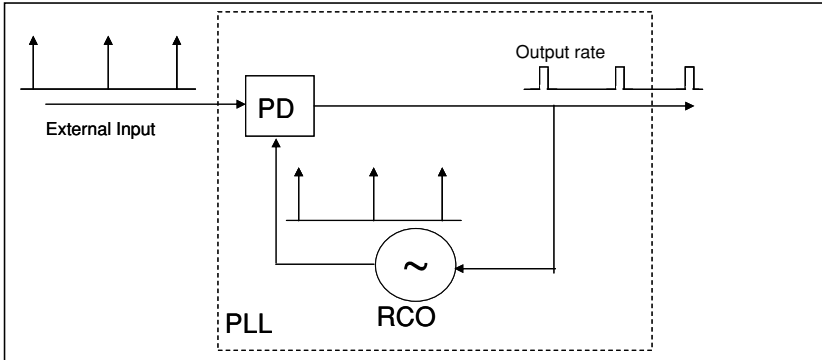
(A)
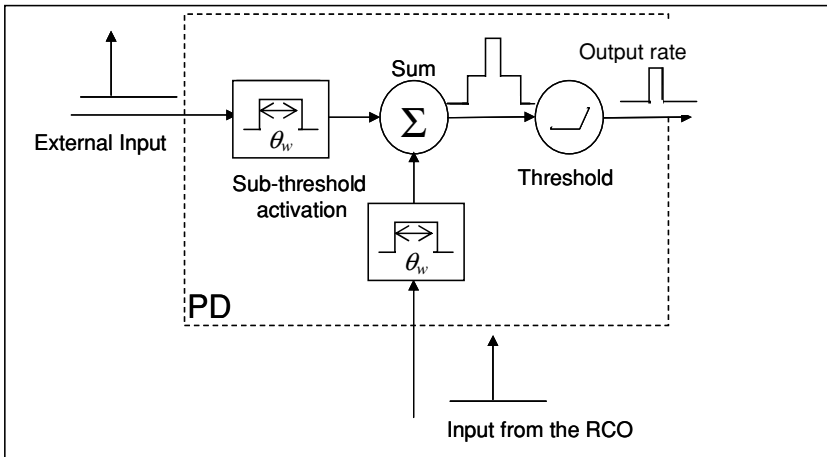
(B)

Figure 1: Neuronal phase-locked loop (NPLL). (A) Schematic illustration of a NPLL, which includes a phase detector (PD) and a rate-controlled oscillator (RCO). (B) Schematic illustration of a particular PD, the subthreshold-activated correlation PD: input events, marked by upward arrows, arrive from either an external source or the internal oscillator and produce subthreshold activation of fixed strength and duration. The subthreshold activations are summed and evoke a fixed-rate response when the threshold is crossed. Thus, the PD responds when the subthreshold activations from both the internal and external sources overlap. Other implementations are discussed in the text and depicted in Figures 2 and 3.

oscillator, the oscillator is reset independent of its history. Thus, the period is assumed to vary only as a function of the phase of the input during the current cycle. Specifically, the instantaneous frequency during the nth cycle is $\dot{\theta}_{osc} = \tau_{osc}^{-1} + h(\theta_{osc}|\{\eta_k\}_{k=N(t_n)+1}^{N(t)})$, where η_k is the time of occurrence of the kth input event, $N(t)$ is the number of input events that occurred up to time t (the counting process; Snyders, 1975), and t_n is the time of occurrence of the nth oscillatory event (and the start of the nth cycle). The function $h(\theta_{osc}|\{\eta_k\}_{k=N(t_n)+1}^{N(t)})$ describes the effect of the input events that occur during the nth cycle and depends in general on their time of occurrence and the phase of the oscillator.

The above effect may be simplified in two extreme but very important cases: pulse-coupled oscillators and rate-controlled oscillators. In the first case, the effect of an isolated input event, usually from a single source, is short compared with the inter-event interval, and in the extreme assumed instantaneous. In the second case, the effects from different input events, coming usually from different sources, are highly overlapping, so the rate rather than the timing of the individual events determines the overall effect.

2.1.1 Pulse-Coupled Oscillators. The instantaneous effect of the input is described by $\dot{\theta}_{osc} = \tau_{osc}^{-1} \pm f(\theta_{osc})\delta(t - \eta_{N(t)})$, where $f(\theta_{osc})$ is known as the phase-response curve (PRC) (Perkel, Schulman, Bullock, Moore, & Segundo, 1964; Kawato & Suzuki, 1978; Winfree, 1980; Yamanishi, Kawato, & Suzuki, 1980; Zacksenhouse, 2001). Upon integration,

$$\theta_{osc} = t/\tau_{osc} \pm \sum_{k=N(t_n)+1}^{k=N(t)} f(\theta_{osc}(\eta_k)),$$

and the perturbed period $\tau_p(n)$ is given by

$$\tau_p(n) = \tau_{osc}\left(1 \mp \sum_{k=N(t_n)+1}^{k=N(t_n+\tau_p)} f(\theta_{osc}(\eta_k))\right).$$

When only one input event occurs during the oscillatory cycle, the modified period is

$$\tau_p(n) = \tau_{osc}\left(1 \mp f(\varphi(n))\right). \tag{2.1}$$

where $\varphi(n) = (\eta_{N(t_n)+1} - t_n)/\tau_{osc}$ is the phase of the oscillator at the time of occurrence of that input event.

As will be further discussed in section 4, a single pulse-coupled oscillator is equivalent to a PLL. However, a PLL may also be implemented by a

(neural) circuit that includes an RCO, whose characteristics are detailed below.

2.1.2 Rate-Controlled Oscillator (RCO).   For simplicity, we assume that the RCO response depends on its input spike rate $r(t)$, independent of its phase, so $\dot{\theta}_{RCO} = \tau_{RCO}^{-1} \pm h_{RCO}(r(t))$, where τ_{RCO} denotes the intrinsic period of the RCO and h_{RCO} describes the effect of the input rate on the instantaneous frequency. Upon integration, the perturbed period is given by

$$\tau_p(n) = \tau_{RCO}\left(1 \mp \int_{t_n}^{t_n + \tau_p} h_{RCO}(r(t))dt\right).$$

This can be expressed in terms of the lumped rate parameter, $R(n)$, which describes the integrated effect of the input to the RCO during its nth cycle on the duration of that cycle, as

$$\tau_p(n) = \tau_{RCO}\big(1 \mp R(n)\big), \quad R(n) = \int_{t_n}^{t_n + \tau_p} h_{RCO}\big(r(t)\big)dt. \tag{2.2}$$

Thus, the lumped rate parameter, $R(n)$, describes the integrated effect of the input during the nth cycle, with the net effect of either shortening or lengthening the period, as denoted by the $\mp$ sign, respectively. These effects are usually associated with excitatory and inhibitory inputs, respectively, although intrinsic currents may cause the reverse effect (Jones, Pinto, Kaper, & Koppel, 2000; Pinto, Jones, Kaper, & Koppel, 2003). In the linear case, that is, linear h_{RCO}, the lumped parameter $R(n)$ is proportional to the total number of spikes that occur during the nth cycle.

The RCO can be implemented by an integrate-and-fire neuron as analyzed and simulated in Zacksenhouse (2001). When the integrate-and-fire RCO is embedded in an inhibitory PLL, the lumped rate parameter is an approximately linear function of the total number of spikes (Zacksenhouse, 2001, equation A8).

An RCO that is embedded in a PLL receives its input from a PD, whose response characteristics are analyzed next.

2.2 Phase Detectors. The PD receives input from two sources, the external input and the internal RCO, and converts the interval between them into an output spike rate. For unique decoding, the conversion should be monotonic, with either a decreasing or increasing response (Ahissar, 1998). In particular, the PD may compute the correlation between the two inputs and respond maximally when the interval is zero (correlation-based PD, or Corr-PD). Alternatively, the PD may compute the time difference between its two inputs and respond minimally when the interval is zero (difference-based PD, or Diff-PD) (Kleinfeld, Berg, & O'Connor, 1999).

2.2.1 Input Representation.   The mathematical formulation of the computation performed by the PD depends on the representation of its input signals, which may be analog, binary, or discrete (Gardner, 1979). Analog signals are described by waveforms (usually sinusoidal) that vary with the phase of the cycle. Binary signals are described by rectangular waveforms whose onset is taken to be the origin. Discrete signals consist of discrete events that occur once per cycle, at a particular phase, which is taken to be the origin. In the context of neural implementations, discrete signals may describe the spike trains from single oscillating neurons, binary signals may describe the spike trains from bursting neurons, and analog signals may describe the average firing rate from a population of neurons and postsynaptic potentials. The main difference between these representations is the information they provide (or do not provide) about the phase variable. Analog signals may provide continuous indication of the phase, while binary and discrete signals provide information only at a specific phase (the origin). (It is noted that binary and discrete signals may be derived from each other and are essentially equivalent. In particular, the zero crossing of the rectangular wave is a discrete signal, and discrete signals may be used to generate rectangular waves using a memory device that is switched on for a fixed duration whenever a discrete event occurs.)

The nature of operation of the PD is directly related to the nature of its inputs. The phase between analog inputs is detected using multiplier circuits, or mixers (Gardner, 1979), which operate as correlation-based PDs. The phase between binary or discrete signals is detected using logical devices (Gardner, 1979), which may operate as either correlation-based PDs (e.g., binary AND-gate) or difference-based PDs (e.g., binary Exclusive-OR gate) (Ahissar, 1998).

Considering the spiking nature of neuronal signaling, we adopt the discrete, or equivalently the binary, representations in this work. These representations facilitate the unified investigation and comparison of PLLs with correlation-based and difference-based PDs. We use the term *event* to reflect either an event in a discrete representation or the rising edge of a rectangular signal in a binary representation.

In the following mathematical formulation, significant phase variables are defined by normalizing the corresponding time intervals with respect to the intrinsic period of the RCO, τ_{RCO}. In particular, each input event is localized with respect to the preceding and the succeeding RCO events, as shown in Figure 2. The normalized intervals between the kth input event and the preceding or succeeding RCO events are referred to as the *phase*, $\varphi(k)$, and *co-phase*, $\psi(k)$, respectively. The normalized intervals since the last input or RCO events are denoted by θ_i and θ_o, respectively. Equation 2.2 describes how the period of the RCO is perturbed by the input it receives from the PD. The external input is composed of two spike trains: (1) a reference spike train described by a free oscillator with period τ_{ip} and normalized input period $\zeta = \tau_{ip}/\tau_{RCO}$, and (2) a novel spike whose timing with respect
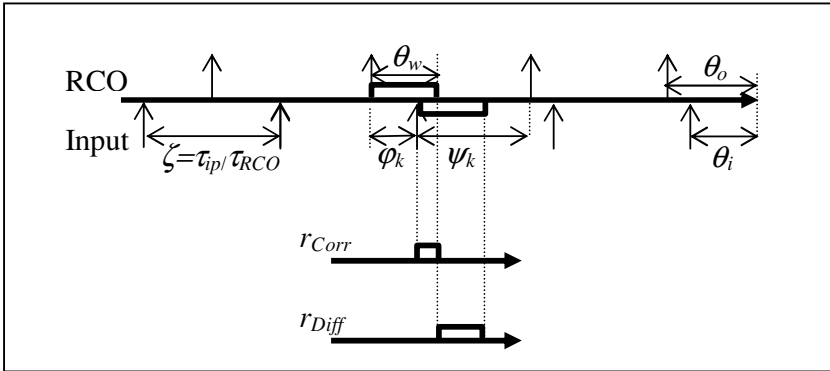
(A)
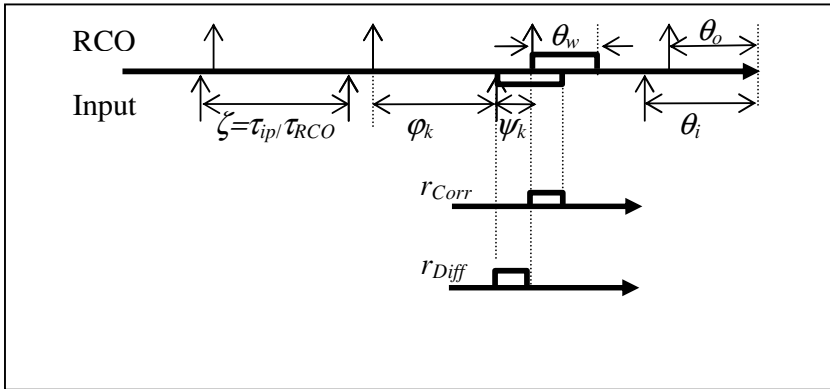
(B)

Figure 2: Phase relationships between input events, marked by upward arrows ending at the horizontal axis, and RCO-generated events, marked by upward arrows originating at the horizontal axis, and the corresponding response of a subthreshold-activated PD. (A, B) Cases in which the input is lagging or leading the RCO events, respectively. The horizontal axes gauge time normalized by the period of the intrinsic RCO, τ_{RCO}, so they correspond directly to the phase. The normalized intervals between the kth input event and the preceding or succeeding RCO events are referred to as the *phase*, $\varphi(k)$, and *co-phase*, $\psi(k)$, respectively. Each event causes a subthreshold activity during a window of normalized duration θ_w, which, for clarity, are marked for only one pair of events in each panel. The resulting responses evoked by that pair of events are depicted on the short axes, for a correlation-based and a difference-based PD, respectively.

to the reference spike train carries the information to be detected by the PLL.

2.2.2 Correlation-based PD.   Two types of simple correlation-based PDs are analyzed in detail and shown to have similar response characteristics, which are then abstracted to characterize the response of general correlation-based PDs.

Simple example of a threshold-activated PD. This is the case depicted in Figure 1B. Each of the inputs to the PD, coming from either the external input or the internal RCO, produces excitatory subthreshold activation for a normalized duration θ_W. The correlation-based PD responds at a constant rate when these activities overlap, as shown schematically in Figure 2. Consequently, the instantaneous output rate of the PD is given by

$$r_{Corr}(\theta_i, \theta_o) = r_0 U(\theta_W - \theta_i) U(\theta_W - \theta_o), \tag{2.3}$$

where r_0 is the constant output rate and $U(\cdot)$ is the unit function (a function that is 1 when its argument is positive and 0 elsewhere). In general, the duration of the subthreshold activation may depend on whether the input is coming from the external input or the internal RCO, but for simplicity of notation, this difference is ignored, and a single θ_W is used.

As derived in equation 2.2, the lumped effect of the PD on the period of the RCO depends on the lumped rate parameter R. Assuming a linear case (and without loss of generality, a unit gain), the lumped rate parameter is given by integrating the instantaneous rate given in equation 2.3. Consequently, an input event that occurs at a phase $\varphi(k)$ and co-phase $\psi(k)$ would result in a lumped rate parameter $R_{corr}(k)$ of

$$R_{corr}(k) = \begin{cases} r_0(\theta_W - \varphi(k)) & \text{if } \varphi(k) < \theta_W \\ r_0(\theta_W - \psi(k)) & \text{if } \psi(k) < \theta_W \text{ .} \\ 0 & \text{otherwise} \end{cases} \tag{2.4}$$

The duration of the subthreshold activation θ_W is assumed to be short enough so at the most, one of the first two conditions holds during regular operation (i.e., $\theta_W < \tau_{RCO}/2$). In the vibrissal system, the duration of individual reference signals, that is, whisking-locked responses of individual first-order trigeminal neurons, is indeed shorter than half of the whisking cycle, and is usually confined to the protraction (forward movement of the whiskers) period (Szwed et al., 2003). When the RCO's period is locked to the whisking period, the above relationship would hold.

Considering the order of input and RCO events that cause the PD to respond, we refer to the first and second cases as input lagging and leading, respectively.
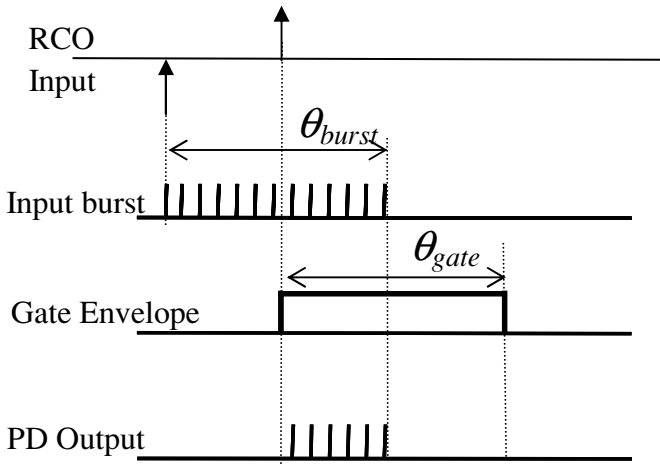
Figure 3: Gated PD. The external input evokes a burst of spikes, which is gated by the PD. The onset of the gating is determined by intrinsic oscillator (RCO).

Simple example of a gated PD. In this case, the external input is composed of a burst of spikes (Szwed et al., 2003), which is gated by the PD, as shown in Figure 3. The onset of the burst is determined by the external input, while the onset of the gating is determined by the RCO. The burst lasts for a normalized duration of θ_{burst} and, for simplicity, is assumed to have a constant rate of r_{ip}. The duration of the gating window is θ_{gate} and for simplicity is assumed to equal the duration of the input burst so $\theta_{gate} = \theta_{burst} \equiv \theta_W$. Thus, the instantaneous output rate of the gated PD is the same as that for the constant rate PD, with $r_0 = r_{ip}$, and equation 2.4 describes the resulting lumped rate parameter due to an isolated external event.

General correlation-based PD. According to equation 2.4, the response of a correlation-based PD decreases linearly with the relevant phase variable (the phase or the co-phase when the input is lagging or leading, respectively). In general, the response may be nonlinear, but its derivative should characteristically be negative:

$$R_{Corr}(k) = \begin{cases} g(\varphi(k)) & \text{if } \varphi(k) < \theta_W \text{ (input lagging)} \\ g(\psi(k)) & \text{if } \psi(k) < \theta_W \text{ (input leading)}, \\ 0 & \text{otherwise} \end{cases} \tag{2.5}$$

where $\dfrac{dg(x)}{dx} \leq 0.$

Equations 2.4 and 2.5 specify the response of a linear or nonlinear correlation-based PD, respectively, to a pair of input and RCO events.

2.2.3 Difference-based PD.   Two types of difference-based PDs, analogous to the ones considered above, are analyzed in detail and shown to have similar response characteristics, which are abstracted to characterize the response of general difference-based PDs.

Simple example of a threshold-activated PD. Here the external input events evoke superthreshold activation of fixed strength and duration, while the RCO events evoke inhibitory activation of a similar strength and duration. The difference-based PD responds at a constant rate when the overall activation is superthreshold, that is, when an external event but not an RCO event occurred during the last window θ_w, as shown schematically in Figure 2. Consequently, the instantaneous output rate is given by

$$r_{Diff}(\theta_i, \theta_o) = r_0 U(\theta_W - \theta_i)U(\theta_o - \theta_W). \tag{2.6}$$

In the linear case considered in the context of the correlation-based PD, the lumped rate parameter is given by:

$$R_{Diff}(k) = \begin{cases} r_0 \varphi(k) & \text{if } \varphi(k) < \theta_W \\ r_0 \psi(k) & \text{if } \psi(k) < \theta_W \\ r_0 \theta_W & \text{otherwise} \end{cases} . \tag{2.7}$$

The window is assumed short enough so at the most, one of the first two conditions, corresponding to input lagging or leading, respectively, holds during regular operation.

Simple example of a gated PD. In this case, the external input involves a burst of spikes, which is relayed by the PD except for the duration of the gate, which blocks the PD response. Using the parameters defined above, the instantaneous output rate of the gated PD is the same as that for the constant rate PD, and equation 2.7 describes the resulting lumped rate parameter due to an isolated external event.

General difference-based PD. According to equation 2.7, the response of a difference-based PD increases linearly with the phase or co-phase in the respective working regions. In general, the response of a difference-based PD may be nonlinear, but its derivative should characteristically be positive:

$$R_{Diff}(k) = \begin{cases} g(\varphi(k)) & \text{if } \varphi(k) < \theta_W & \text{(input lagging)} \\ g(\psi(k)) & \text{if } \psi(k) < \theta_W & \text{(input leading)}, \\ g(\theta_W) & & \text{otherwise} \end{cases} \tag{2.8}$$

where $\dfrac{dg(x)}{dx} \geq 0$.

Table 1: PLL Characterization.

	Correlation-Based PD		Difference-Based PD	
	ePLL ($\zeta \leq 1$)	iPLL ($\zeta \geq 1$)	ePLL ($\zeta \leq 1$)	iPLL ($\zeta \geq 1$)
Input Relevant phase	Lagging Phase φ	Leading Co-phase ψ	Leading Co-phase ψ	Lagging Phase φ
Steady phase	$\varphi_\infty =$ $g^{-1}[(1-\zeta)]$	$\psi_\infty =$ $g^{-1}[(\zeta-1)]$	$\psi_\infty =$ $g^{-1}[(1-\zeta)]$	$\varphi_\infty =$ $g^{-1}[(\zeta-1)]$
Linear case	$\varphi_\infty =$ $\frac{r_0\theta_w-1+\zeta}{r_0}$	$\psi_\infty =$ $\frac{r_0\theta_w+1-\zeta}{r_0}$	$\psi_\infty = \frac{1-\zeta}{r_0}$	$\varphi_\infty = \frac{-1+\zeta}{r_0}$
As $\zeta \to 1$	$\varphi_\infty \uparrow$	$\psi_\infty \uparrow$	$\psi_\infty \downarrow$	$\varphi_\infty \downarrow$

Equations 2.7 and 2.8 specify the response of a linear or nonlinear difference-based PD, respectively, to a pair of input and RCO events.

2.3 PLL Stable Response. During stable 1:1 phase entrainment to a periodic, external input, the response of the PD (and thus of the PLL) is sensitive to either the phase or the co-phase depending on the type of the PD and its connection to the RCO. A PLL in which the PD connection to the RCO is excitatory is referred to as an *excitatory PLL* (ePLL), while a PLL in which the PD is connected to the RCO via an inhibitory interneuron is referred to as an *inhibitory PLL* (iPLL) (Ahissar, 1998). The following theorem characterizes the operation of the different PLLs and is summarized in Table 1.

Theorem 1: PLL Characterization. *During stable 1:1 entrainment of ePLL/ iPLL, the input is lagging or leading, respectively, when the PD is correlation based, and leading or lagging, respectively, when the PD is difference based. Within the working range (i.e., $\zeta \leq 1$ or $\zeta \geq 1$), as the input period approaches the intrinsic period of the RCO, the corresponding phase variable, that is, the steady-state phase φ_∞ for lagging input or the steady-state co-phase ψ_∞ for leading input, increases when the PD is correlation based and decreases when the PD is difference based.*

Proof.   Considering an interval of time during which the input is consistently lagging (i.e., $\varphi(k) < \theta_W$ for all the input events in the interval), the phase of the $(k+1)$th input is related to the phase of the kth input by $\varphi(k+1) = \varphi(k) + \zeta - \tau_p(k)/\tau_{RCO}$. According to equation 2.2 and either equation 2.5 or 2.8, the perturbed period is given by

$$\tau_p(k)/\tau_{RCO} = 1 \mp g(\varphi(k)), \tag{2.9}$$

regardless of the type of the PD, so

$$\varphi(k+1) = \varphi(k) + \zeta - 1 \pm g(\varphi(k)). \tag{2.10}$$

When the input is consistently leading $\psi(k) < \theta_W$, the co-phase of the $(k+1)$th input is related to the co-phase of the kth input by $\psi(k+1) = \psi(k) - \zeta + \tau_p/\tau_{RCO}$. According to equation 2.2 and either equation 2.5 or 2.8, the perturbed period is given by

$$\tau_p(k)/\tau_{RCO} = 1 \mp g(\psi(k)), \tag{2.11}$$

regardless of the type of the PD, so

$$\psi(k+1) = \psi(k) - \zeta + 1 \mp g(\psi(k)). \tag{2.12}$$

Equations 2.10 and 2.12 imply that the equilibrium condition is specified by $\varphi_\infty = g^{-1}[\pm(1-\zeta)]$ when the input is lagging and by $\psi_\infty = g^{-1}[\pm(1-\zeta)]$ when the input is leading. Furthermore, the stability condition is given by $-2 < \pm\frac{dg(x)}{dx}|_{\varphi_\infty} < 0$ when the input is lagging and by $-2 < \mp\frac{dg(x)}{dx}|_{\psi_\infty} < 0$ when the input is leading. For the correlation-based PD, $dg/dx \leq 0$ so the ePLL stabilizes with lagging input at $\varphi_\infty = g^{-1}[(1-\zeta)]$ and the iPLL stabilizes with leading input at $\psi_\infty = g^{-1}[\zeta-1]$. For the difference-based PD, $dg/dx \geq 0$, so the opposite holds.

The period of the input to an ePLL is shorter than the intrinsic period of the RCO so $\zeta \leq 1$. As the frequency of the input approaches the intrinsic frequency of the RCO, $\zeta \uparrow 1$, so $(1-\zeta) \downarrow 0$. The period of the input to an iPLL is longer than the intrinsic period of the RCO, so $\zeta \geq 1$. As the frequency of the input approaches the intrinsic frequency of the RCO, $\zeta \downarrow 1$ so $(\zeta-1) \downarrow 0$. For a correlation-based PD, $dg/dx \leq 0$, and so both the steady phase φ_∞ and the steady co-phase ψ_∞ increase as the frequency of the input approaches the intrinsic frequency of the RCO from below or above for the ePLL/iPLL, respectively. For the difference-based PD, $dg/dx \geq 0$ so both the steady phase φ_∞ and the steady co-phase ψ_∞ decrease as the frequency of the input approaches the intrinsic frequency of the RCO from below or above for the ePLL/iPLL, respectively.

The linear operating curves of the different PLLs, given in Table 1, are depicted in Figure 4 in terms of the absolute delay as a function of the input period. The different panels depict the effect of the nominal rate r_0, and the parallel curves within each panel depict the effect of the intrinsic period τ_{RCO}. It is noted that the operating range increases as the nominal rate increases. However, according to the proof of the PLL characterization theorem, r_0 should be less than 2 to ensure stability, so only the top panels depict stable (top left) and marginally stable (top right) operating curves.
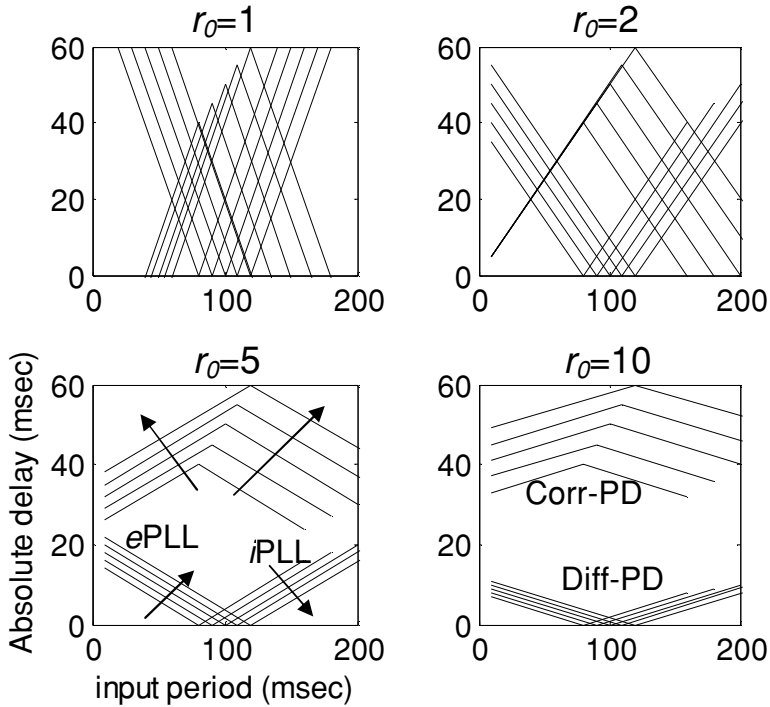
Figure 4: Linear steady-state curves describing the absolute delay between the external input and internal oscillatory events as a function of the input period for four types of PLLs. The curves shift in parallel as the intrinsic rate of the RCOs is increased from 80 to 120 msec in steps of 10 msec as indicated by the arrows in the bottom left panel. The nominal rate r_0 is 1 (top left panel), 2 (top right panel) 5 (bottom left panel), and 10 (bottom right panel).

Based on the PLL characterization theorem, we can classify the PLLs into two groups according to whether they are sensitive to the phase or co-phase of the input relative to the intrinsic oscillator. The phase-sensitive PLLs include (a1) the ePLL with correlation-based PD and (a2) the iPLL with difference-based PD, while the co-phase-sensitive PLLs include (b1) the iPLL with a correlation-based PD and (b2) the ePLL with a difference-based PD.

3 Temporal Decoding

3.1 Vibrissal Temporal Decoding Task. The entrainment of the PLL by a periodic input prepares the PLL to properly decode a novel input. In order to clarify this subtle issue, we consider in more detail the encoding of object

Table 2: Total Response R_t of Phase-Locked NPLLs to a Novel Input.

	Correlation-Based PD		Difference-Based PD	
	ePLL	iPLL	ePLL	iPLL
Novel Input/RCO Event				
Leading (ψ_n)	$g(\varphi_\infty) + g(\psi_n)$	$g(\psi_\infty) + g(\psi_n)$	$g(\psi_\infty) + g(\psi_n)$	$g(\varphi_\infty) + g(\psi_n)$
Lagging (φ_n)	$g(\varphi_\infty) + g(\varphi_n)$	$g(\psi_\infty) + g(\varphi_n)$	$g(\psi_\infty) + g(\varphi_n)$	$g(\varphi_\infty) + g(\varphi_n)$
Linear PD				
Leading (ψ_n)	$r_0[2\theta_w - (\varphi_\infty + \psi_n)]$	$r_0[2\theta_w - (\psi_\infty + \psi_n)]$	$r_0(\psi_\infty + \psi_n)$	$r_0(\varphi_\infty + \psi_n)$
Lagging (φ_n)	$r_0[2\theta_w - (\varphi_\infty + \varphi_n)]$	$r_0[2\theta_w - (\psi_\infty + \varphi_n)]$	$r_0(\psi_\infty + \varphi_n)$	$r_0(\varphi_\infty + \varphi_n)$

location in the vibrissal system. The location of the object is encoded in the firing pattern of neurons in the trigeminal ganglion and probably also in the brainstem. In particular, the firing patterns of trigeminal neurons, which provide the external input to the vibrissal system, include two components (Kleinfeld et al., 1999; Szwed et al., 2003): (1) a reference signal composed of spikes at a preferred phase of the whisking cycle and (2) a contact-induced signal composed of spikes that are evoked on contact with an external object. The first component is periodic at the whisking period. The second component is the novel input whose time of occurrence relative to the reference signal (the first component) has to be decoded.

3.2 Effect of Novel Input. The external input to the PD is composed of two components: the reference, periodic input, and the novel input. We make the simple and physiologically appropriate assumption that the PD's response to each of these components is the same and independent of each other, so the total response of the PD is the sum of the individual responses. For the gated PD described in section 2.2.3, for example, once the gate is opened by the RCO, the PD relays the bursts of activity that it receives from either or both of the external inputs. Using equations 2.4, 2.5, 2.7, and 2.8 for the response to either component of the external input, the total response R_t of the different NPLLs can be derived as summarized in Table 2 and depicted in Figure 5.

As evident from Table 2 and Figure 5, the total PD response varies monotonically with the delay between the novel input and the oscillatory event (i.e., φ_n or ψ_n) as long as the novel input is confined to either always lead or always lag the RCO event. However, in order to provide sensory decoding, the response should vary monotonically with the delay between the novel input and the reference events. The relevant decoding ranges are specified by the temporal detection theorem stated and proven in the next section.
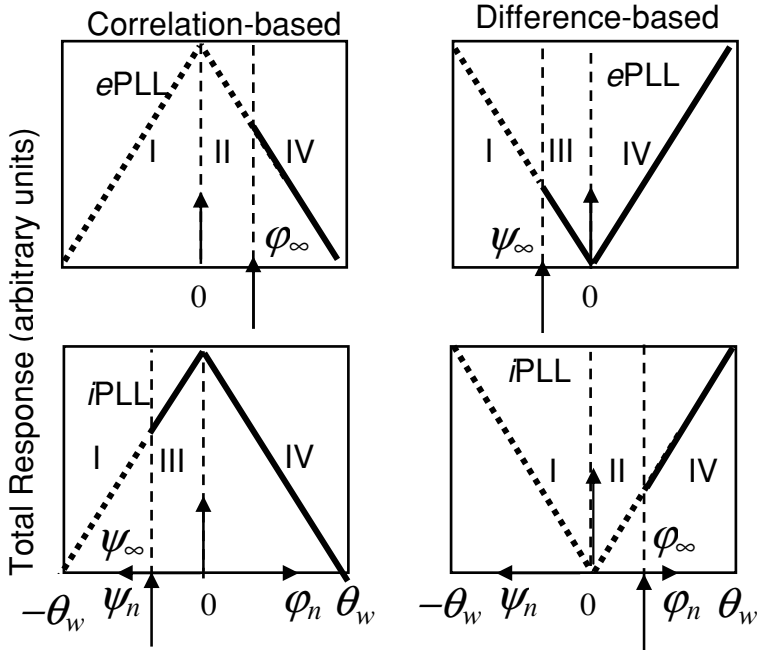
Figure 5: Total PD response as a function of the phase φ_n (increasing to the right) and co-phase ψ_n (increasing to the left) of a novel input to a PLL that is entrained by a periodic reference input with the indicated phase φ_∞ or co-phase ψ_∞ relationship. The left/right pair of panels depict the total response of correlation-/difference-based PDs embedded in ePLL (upper panels) and iPLL (bottom panels). The arrows below the axes indicate the reference input, while the arrows above the axes indicate the RCO events. The roman numbers indicate the corresponding zone of the novel input as indicated in Table 2. The solid/dashed lines indicate the response when the novel input lags/lead the reference input.

3.3 PLL Temporal Decoding Capabilities

Theorem 2: PLL Temporal Detection.   *During 1:1 stable phase locking to a periodic external input, a PLL can monotonically decode a novel input when it has a fixed order with respect to both the reference input and the RCO events. The resulting decoding ranges are specified in Table 3.*

Proof.   The output of the PD varies monotonically with the phase of the novel input along the RCO cycle as long as the order between them is fixed (second column of Table 3). The phase difference between the novel input

Table 3: Monotonic Decoding Ranges.

Novel Input/ Reference Input	Novel Input/ RCO Events	Zone (Figure 5)	Correlation-Based PD		Difference-Based PD	
			ePLL	iPLL	ePLL	iPLL
Leading	Leading	I	θ_W	$\theta_W - \psi_\infty$	$\theta_W - \psi_\infty$	θ_W
Leading	Lagging	II	φ_∞	0	0	φ_∞
Lagging	Leading	III	0	ψ_∞	ψ_∞	0
Lagging	Lagging	IV	$\theta_W - \varphi_\infty$	θ_W	θ_W	$\theta_W - \varphi_\infty$

and the reference input varies monotonically with the phase of the novel input along the cycle of the RCO as long as the order between them is fixed (first column of Table 3). Hence, the response of the PD varies monotonically with the phase difference between the novel input and the reference input when the order of the novel input with respect to both the reference input and the RCO events is fixed, as specified by each row. Finally, the relevant ranges with the specified phase relationships between the novel input and both the reference input (first column of Table 3) or the RCO events (second column of Table 3) follow directly given the steady-state phase and co-phase of the reference input with respect to the RCO events.

It is apparent that the decoding range depends on whether the PLL is phase or co-phase sensitive. When the order between the novel input and the reference input is determined by the nature of the temporal decoding task, it is possible to distinguish between two decoding modes: (1) narrow but monotonic, and thus unambiguous, decoding range (e.g., correlation-based ePLL decoding a novel input that lags the reference input over the range $\theta_w - \varphi_\infty$; bottom row of the third column in Table 3; see also the top-left panel in Figure 5), and (2) wide but partially ambiguous detection range (e.g., a correlation-based iPLL decoding a novel input that lags the reference input over the range $\theta_w + \varphi_\infty$; bottom two rows of the fourth column in Table 3; see also the bottom-left panel in Figure 5). The ambiguity stems from the fact that the order of the novel input with respect to the RCO events is not constrained in this case. Thus, the temporal detection theorem provides a design criterion for selecting the PLL that best matches the requirements of a given temporal decoding task.

The sensory information is encoded in the phase difference δ between the novel input and the reference input and can be expressed in terms of the phase of the novel input with respect to the closest RCO event and the phase of the reference input with respect to the same RCO event, as specified in Table 4. The following PLL temporal decoding theorem specifies how this informative phase difference may be determined from the response of the PD.

Table 4: Phase Difference δ Between the Novel Input and the Reference Input.

Novel Input/Reference Input	Novel Input/ RCO Events	Phase-Sensitive PLLs	Co-Phase-Sensitive PLLs
Leading	Leading (ψ_n)	$\varphi_\infty + \psi_n$	$\psi_n - \psi_\infty$
Leading	Lagging (φ_n)	$\varphi_\infty - \varphi_n$	NA
Lagging	Leading (ψ_n)	NA	$\psi_\infty - \psi_n$
Lagging	Lagging (φ_n)	$\varphi_n - \varphi_\infty$	$\psi_\infty + \varphi_n$

Table 5: Parameters of the Relationship $\delta = a + b\,R_\infty/r_0 + c\,R_t/r_0$ Specifying the Phase Difference δ Between the Novel Input and the Reference Input as a Function of the Steady-State PD Response (R_∞) and Total Response (R_t) of the PD.

Novel Input/Reference Input	Novel Input/RCO Events	Correlation-Based PD		Difference-Based PD	
		ePLL	iPLL	ePLL	iPLL
Leading	Leading (ψ_n)	$a = 2$; $b = 0$; $c = -1$	$a = 0$; $b = 2$; $c = -1$	$a = 0$; $b = -2$; $c = 1$	$a = 0$; $b = 0$; $c = 1$
Leading	Lagging (φ_n)	$a = 0$; $b = -2$; $c = 1$	NA	NA	$a = 0$; $b = 2$; $c = -1$
Lagging	Leading (ψ_n)	NA	$a = 0$; $b = -2$; $c = 1$	$a = 0$; $b = 2$; $c = -1$	NA
Lagging	Lagging (φ_n)	$a = 0$; $b = 2$; $c = -1$	$a = 2$; $b = 0$; $c = -1$	$a = 0$; $b = 0$; $c = 1$	$a = 0$; $b = -2$; $c = 1$

Theorem 3: PLL Temporal Decoding.   *Consider a PLL that is phase-locked to a periodic reference signal, and denote by R_∞ the steady-state response of its PD. A novel input induces an additional response so the total response of the PD is given by R_t. The phase difference δ between the novel input and the reference input may be determined by $\delta = a + b\,R_\infty/r_0 + c\,R_t/r_0$ with the parameters given in Table 5 for the specific PLL variant.*

Proof.   The PLL decoding theorem follows directly from Tables 4 and 3 after expressing the steady-state phase or co-phase in terms of the steady response R_∞ using equations 2.4 and 2.7.

It is noted that in some cases, the computation involves the steady-state PD response R_∞. This may be made available by PLLs that do not receive the novel input and thus continue to respond at R_∞ even when the novel input appears. However, when operating in the regime for which the specific

PLL variant has the maximum decoding range (as specified in Table 2), the steady-state PD response is not required. Specifically, when the novel input lags both the RCO event and the reference event, the phase difference δ may be directly inferred from the PD response of the co-phase-sensitive PLLs (e.g., an iPLL with a correlation-based PD) after an appropriate offset.

3.4 Significance for Vibrissal Temporal Decoding.

3.4.1 Decoding Range.   The whisking-locked reference signal is evoked upon the onset of the protraction phase of whisking, that is, the phase of forward movement, while the contact-induced signal is evoked later during protraction, upon contact with the object (Szwed et al., 2003). Thus, the contact-induced novel input lags the whisking-induced reference input. According to the temporal detection theorem, the decoding ranges that can be achieved in this case by the different PLL variants are specified in the last two rows of Table 2. In particular, the phase-sensitive PLLs (i.e., the ePLL with correlation-based PD and the iPLL with difference-based PD; zone IV, solid curves in the upper-left and lower-right panels of Figure 5) result in an unambiguous but narrow decoding range, while the co-phase-sensitive PLLs (i.e., the iPLL with correlation-based PD and the ePLL with difference-based PD; zones III and IV, solid curves in Figure 5 lower-left and upper-right panels) result in a wide but partially ambiguous decoding range.

In the latter case, the response is ambiguous when the novel input lags the reference input by less than twice the co-phase ψ_∞, that is, when the contact with the object occurs relatively close to the preferred phase of the whisking cycle. However, the response is still informative since it provides approximate indication of the phase of the novel input, and furthermore, it can be resolved by considering the response from a population of PLLs that receive reference signals produced at different preferred phases (Ahissar, 1998). Hence, it can be concluded that in the case of vibrissal temporal decoding, the widest detection and decoding ranges are obtained with co-phase-sensitive PLLs, for which the input leads the intrinsic oscillator during stable entrainment, in agreement with the observed oscillatory delay (Nicolelis et al., 1995; Ahissar et al., 1997).

The two co-phase-sensitive PLLs, that is, the iPLL with a correlation-based PD and the ePLL with a difference-based PD, differ in their input operating ranges, which include input periods that are longer or shorter than the intrinsic period of the oscillator, respectively (see Table 1, first row). Recordings from whisking-range oscillatory neurons in the somatosensory cortex indicate that they track mainly frequencies below their spontaneous frequency (Ahissar et al., 1997). Thus, given the above theorems, the observations suggest that the somatosensory cortex participates in the implementation of iPLLs with correlation-based PDs.

3.4.2 Frequency Modulation Experiments.   Additional support for the above conclusion may be drawn from frequency modulation experiments in which the whiskers are stimulated by air puffs whose frequency is modulated by a slowly varying sinusoidal signal. The responses of neurons along the paralemniscal pathway (one of the two major vibrissal sensory pathways) followed the oscillatory input with varying latencies and spike counts. As the frequency of the input varied sinusoidally between 3 and 7 Hz at a modulating frequency of 0.5 Hz, so did the latency and the spike count of these neurons. However, while the first varied in phase with the frequency of the stimulus, the latter varied in antiphase (Ahissar et al., 2000; Ahissar, Sosnik, Bagdasarian, & Haidarli, 2001).

In particular, the latencies and spike counts of cortical neurons in layer 5a, which receive input from thalamic neurons in the medial division of the posterior nucleus (POm) along the paralemniscal pathway, were inversely related, as plotted in Figure 6 (connected stars). Under the hypothesis that the thalamocortical loops in the vibrissal paralemniscal system implement NPLLs, the thalamic neurons should act as PDs (Ahissar et al., 1997). According to section 2.2.2, the observed relationship in neurons of layer 5a indicates that the thalamic neurons that drive these cortical neurons behave as correlation-based PDs. Thus, considering the four possible PLL variants, the observed latencies and inverse relationship are consistent only with the assumption that the paralemniscal pathway implements *i*PLLs with correlation-based PDs, in agreement with our previous conclusion.

Indeed, simulations of an *i*PLL with a correlation-based PD demonstrate a similar relationship, as shown in Figure 6. The circles in Figure 6 depict the relationship between the spike count and the latency of the response of the simulated PD to a frequency-modulated spike train input. To facilitate comparison, the linear fit to the measured data is marked by a dashed line, demonstrating good agreement with the simulated results.

4 Single Neural Oscillators

A single neuron can also be modeled as a PLL (Hoppensteadt, 1986). However, as indicated by equation 2.1, single neural oscillators are sensitive to the phase at which the input events occur, not the co-phase. This is indeed the basis for characterizing neural oscillators using phase-response curves. In particular, a single neural oscillator, described by equation 2.1, is equivalent to a PLL with lagging input as described by equation 2.9, where $f(\varphi) = g(\varphi)$. However, a single neural oscillator cannot operate as a NPLL with leading input, as described by equation 2.11, since its dynamics depends on only the phase, never the co-phase, of the input.

As discussed above, the PLL temporal detection theorem suggests that single oscillators, which can be sensitive only to the phase but not to the co-phase, would provide a narrow decoding range when the novel input
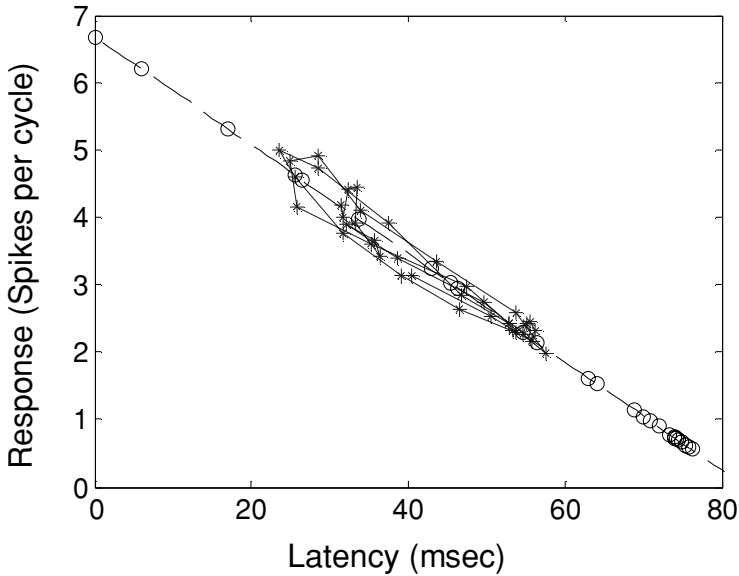
Figure 6: Average spike count versus average latency of paralemniscal corti-
cal neurons recorded from layer 5a of the barrel cortex in experiments with
frequency modulated (FM) stimulus (Ahissar et al., 2000; Ahissar et al., 2001).
Data points are marked with stars, each representing the latency and spike count
for one cycle, averaged across 36 repetitions of the same FM sequence (first cycle
excluded). Results from consecutive cycles are connected by a solid line. The
dashed line is a linear fit to the data with a slope of -0.08, and the circles are
generated from a simulated iPLL with correlation-based PD in response to a
frequency-modulated input spike train.

lags the reference input. Hence, we conclude that single oscillators are not
optimal for temporal decoding of the whisking-induced signals.

Since single neurons can be sensitive only to the phase, and not the co-
phase, of the external input, the PLL characterization theorem implies that
they can implement either ePLL with correlation-based PD or iPLL with
difference-based PDs. To be able to track frequencies below their sponta-
neous frequency (Ahissar et al., 1997), the single neurons should operate as
iPLL with difference-based PDs.

5 Summary and Discussion

5.1 Temporal Decoding Tasks. In the context of neural information
processing, temporal decoding refers to the ability to respond in a way that
is sensitive to the temporal pattern of neural activity, not just its average

spike rate. This article addresses a specific temporal decoding task, which is sensitive to the relative phase of an information-carrying signal (spike train) relative to a periodic reference signal (periodic spike train). Phase-decoding capabilities facilitate the interpretation of neural activity evoked during active touch or active vision (Ahissar & Arieli, 2001). In such active processes, the controlled movements of the sensory organs evoke the reference spike train, while the sensed features of the environment evoke the information-carrying signal. During whisking, for example, the sensory organs are the flexible whiskers, which scan the environment rhythmically, and the relevant feature is the position of an object in that environment. The angle of contact, and thus the relative angular position of the object, can be inferred from the phase along the whisking cycle at which the contact occurred.

5.2 Temporal Decoding Capabilities of PLLs. PLLs are well-developed electronic circuits designed to track periodic signals over a wide frequency range with good noise-rejection performance. The output of the internal oscillator reproduces a cleaned version of the original signal, while the PD followed by a low-pass filter demodulates the input signal.

Similarly, neuronal PLLs may be used to track the period of the input spike train and encode its variations in the output—the number of spikes per cycle—of the PD. In this mode, the sensitivity of the PLL may be defined as the change in the output of the PD induced by a small change in the period of the input. Previous work (Zacksenhouse, 2001) indicates that the sensitivity of the iPLL is relatively constant compared with the sensitivity of single-neuron oscillators.

By tracking the frequency of the input, PLLs can also be used to detect the relative phase of a novel input, and thus accomplish the phase-decoding task, which is critical for the interpretation of active sensation, as discussed above. Specifically, the PD decodes the phase of the novel input with respect to the periodic activity of the internal oscillator. However, the internal oscillator of an entrained PLL is phase-locked to the reference input, and so the PLL indirectly decodes the phase of the novel input with respect to that reference spike train. The performance of PLLs with respect to this task is the focus of this article.

The four PLL variants, involving correlation- and difference-based PDs with either inhibitory (iPLL) or excitatory (ePLL) connections, operate in two locking modes, which are sensitive to either the phase or co-phase of the input. In particular, the iPLL with correlation-based PD and the ePLL with difference-based PD are sensitive to the co-phase of the input, and thus establish a unique response pattern that cannot be produced by single-neuron oscillators. The operating range over which the timing of the novel input may be decoded with respect to the reference signal has been determined and provides a design criterion for selecting the optimum PLL variant that best matches the requirements for a given task.

5.3 Circuit-Based versus Single-Neuron PLLs. The relationship between the operation of a single neuron and that of a phase-locked loop was suggested and extensively explored in Hoppensteadt (1986). The cell body is modeled as a voltage-controlled oscillator (VCO, equivalent to RCO here), and the synaptic effect as a monotonically increasing nonlinear function of the combined effect of the VCO and the external input. The resulting model was shown here to be equivalent to either iPLL with a difference-based PD or ePLL with correlation-based PD.

5.4 Temporal Decoding in the Vibrissal System. The hypothesis that temporal decoding in the vibrissal system is facilitated by neural circuits implementing PLLs has received substantial support from a range of observations: (1) existence of neural oscillators in the relevant range of frequencies (Ahissar et al., 1997), (2) existence of PD-like neurons, which exhibit frequency-dependent gated outputs (Ahissar et al., 2000), (3) phase locking of oscillators and PD-like neurons to a range of input frequencies (Ahissar et al., 1997), (4) monotonic direct relationships between input frequencies to locking phases in both oscillators and PD-like neurons (Ahissar et al., 2000), (5) monotonic inverse relationships between input frequencies to locking spike counts in PD-like neurons (Ahissar et al., 2000), which depend on the length of the stimulus burst (Ahissar et al., 2001; Sosnik et al., 2001), and (6) estimated sensitivity that agrees with the observed marginal stability (Zacksenhouse, 2001). In this article, we provide additional theoretical support for this hypothesis based on the decoding range of the different PLL variants. The nature of the temporal decoding task facing the vibrissal system suggests that the widest detection and decoding ranges may be achieved with the co-phase-sensitive PLLs, and those cannot be implemented by single neural oscillators. Furthermore, new observations from frequency-modulated experiments are described that support the hypothesis that the vibrissal system implements iPLLs with correlation-based PDs.

Control Capabilities of PLLs. Neural oscillators play an important role not only in decoding but also in generating temporal patterns (Zacksenhouse, 2001). In particular, networks of coupled oscillators are assumed to generate patterns of rhythmic movements that underlie a diverse range of rhythmic tasks, including locomotion (Nishii, Uno, & Suzuki, 1994; Rand et al., 1986) and chewing (Rowat & Selverston, 1993), for example. These networks can generate the patterns of activity even in the absence of any sensory feedback, and thus are referred to as central pattern generators (CPGs). However, feedback may still play an important role in these tasks (Ekeberg, 1993; Grillner et al., 1995) and in particular in tasks that involve open-loop unstable dynamical systems.

The closed-loop control of such tasks, and in particular the control of yoyo-playing with oscillatory units, revealed additional advantages of PLLs over single-neuron oscillators (Jin & Zacksenhouse, 2002, 2003). In

this application, the neural oscillator determines when to start the upward movement and receives a once-per-cycle input at a characteristic phase of the movement, when the yoyo reaches the bottom of its flight. As discussed here, single neural oscillators, or single-cell PLLs, may establish only input-lagging phase relationships, while neural network PLLs may also establish a unique input-leading phase relationship. The latter was demonstrated to have critical control advantages, which are essential in the context of yoyo playing (Jin & Zacksenhouse, 2002, 2003). Thus, the unique temporal detection characteristics of circuit PLLs also provide control capabilities beyond those of directly coupled neural oscillators.

Acknowledgments

References

Ahissar, E. (1998). Temporal-code to rate-code conversion by neuronal phase-locked loops. *Neural Comput., 10*, 597–650.

Ahissar, E., & Arieli, A. (2001). Figuring space by time. *Neuron, 22*, 185–201.

Ahissar, E., Haidarliu, S., & Zacksenhouse, M. (1997). Decoding temporally encoded sensory input by cortical oscillations and thalamic phase comparators. *Proc. Natl. Acad. Sci. USA, 94*, 11633–11638.

Ahissar, E., Sosnik, R., Bagdasarian, K., & Haidarliu, S. (2001). Temporal frequency of whisker movement, II. Laminar organization of cortical representations. *J. Neurophysiol, 86*, 354–367.

Ahissar, E., Sosnik, R., & Haidarliu, S. (2000). Transformation from temporal to rate coding in somatosensory thalamocortical pathway. *Nature, 406*, 302–305.

Ahissar, E., & Vaadia, E. (1990). Oscillatory activity of single units in a somatosensory cortex of an awake monkey and their possible role in texture analysis. *Proc. Natl. Acad. Sci. USA, 87*, 8935–8939.

Ahissar, E., & Zacksenhouse, M. (2001). Temporal and spatial coding in the rat vibrissal system. *Prog. in Brain Res., 130*, 75–87.

Amitai, Y. (1994). Membrane potential oscillations underlying firing patterns in neocortical neurons. *Neuroscience, 63*, 151–161.

Ekeberg, O. (1993). A neuro-mechanical model of undulatory swimming. *Biol. Cybern., 69*, 363–374.

Flint, A. C., Maisch, U. S., & Kriegstein A. R. (1997). Postnatal development of low [Mg2+] oscillations in neocortex. *J. Neurophysiol.*, 78, 1990–1996.

Gardner, F. M. (1979). *Phaselocked techniques* (2nd ed.) New York: Wiley.

Grillner, S., Deliagina, T., Ekeberg, O., El Manira, A., Hill, R. H., Lansner, A., Orlovsky, G. N., & Wallen, P. (1995). Neural-networks that co-ordinate locomotion and body orientation in the lamprey. *Trends Neurosci., 18*, 270–279.

Hoppensteadt, F. C. (1986). *An introduction to the mathematics of neurons.* Cambridge: Cambridge University Press.

Jin H., & Zacksenhouse, M. (2002). Necessary condition for simple oscillatory neural control of robotic yoyo. In *Int. Joint Conf. on Neural Networks, World Cong. on Intell. Comp. (IJCNN-WCCI'02)* (pp. 1427–1432). Honolulu, HI.

Jin, H., & Zacksenhouse, M. (2003). Oscillatory neural control of dynamical systems. *IEEE Trans. Neural Networks, 14*(2), 317–325.

Jones, S. R., Pinto, D. J., Kaper, T. J., & Koppel, N. (2000). Alpha-frequency rhythms desynchronize over long cortical distances: A modeling study. *J. Comp. Neurosci., 9*, 271–291.

Kawato, M., & Suzuki, R. (1978). Biological oscillators can be stopped—topological study of a phase response curve. *Biol. Cybern. 30*, 241–248.

Kleinfeld, D., Berg, R. W., & O'Connor, S. M. (1999). Anatomical loops and their electrical dynamics in relation to whisking by rat. *Somatosensory and Motor Res., 16*(2), 69–88.

Lebedev, M. A., & Nelson, R. J. (1995). Rhythmically firing (20–50 Hz) neurons in monkey primary somatosensory cortex: Activity patterns during initiation of vibratory-cued hand movements. *J. Comp. Neurosci., 2*, 313–334.

Marr, D. (1982). *Vision: A computational investigation into the human representation and processing of visual information*. New York: Freeman.

Nicolelis, M. A. L., Baccala, L. A., Lin, R. C. S., & Chapin, J. K. (1995). Sensorimotor encoding by synchronous neural ensemble activity at multiple levels of the somatosensory system. *Science, 268*, 1353–1358.

Nishii, J., Uno, Y. & Suzuki, R. (1994). Mathematical models for the swimming pattern of a lamprey I and II. *Biol. Cybern., 72*, 1–9, 11–18.

Perkel, D. H., Schulman, J. H., Bullock, T. H., Moore, G. P. & Segundo J. P. (1964). Pacemaker neurons: Effects of regularly spaced synaptic input. *Science, 145*, 61–63.

Pinto, D. J., Jones, S. R., Kaper, T. J., & Koppel, N. (2003). Analysis of state-dependent transitions in frequency and long-distance coordination in a model oscillatory cortical circuit. *J. Comp. Neurosci.*, 15, 283–298.

Rand, R. H., Cohen, A. H., & Holmes, P. J. (1986). Systems of coupled oscillators as models of central pattern generators. In A. H. Cohen, S. Rossignol, and S. Grillner (Eds.), *Neural control of rhythmic movements in vertebrates*. New York: Wiley.

Rowat P. F., & Selverston, A. I. (1993). Modeling the gastric mill central Pattern generator of the lobster with a relaxation-oscillator Network. *J. Neurophysiol., 70*(3), 1030–1053.

Silva, L. R., Amitai, Y., & Connors, B. W. (1991). Intrinsic oscillations of neocortex generated by layer 5 pyramidal neurons. *Science, 251*, 432–435.

Sosnik, R., Haidarliu, S., & Ahissar, E. (2001). Temporal frequency of whisker movement. I. Representations in brainstem and thalamus. *J. Neurophysiol., 86*, 339–353.

Snyders, D. L. (1975). *Random point processes*. New York: Wiley.

Szwed, M., Bagdasarian, K., and Ahissar, E. (2003). Encoding of vibrissal active touch. *Neuron, 40*, 621–630.

Winfree, A. T. (1980). *Geometry of biological time*. Berlin: Springer.

Yamanishi, J., Kawato, M., & Suzuki, R. (1980). Two coupled oscillators as a model for the coordinated finger tapping by both hands. *Biol. Cybern., 37*, 219–225.

Zacksenhouse, M. (2001). Sensitivity of basic oscillatory mechanisms for pattern generation and detection. *Biol. Cybern., 85*(4), 301–311.